FUNDAMENTAL AND EXPLORATORY RESEARCH

Ernest L. Majer

510/486-6709
elmajer@lbl.gov

The Fundamental and Exploratory Research Program (FERP) covers fundamental earth sciences research conducted in support of the Department of Energy's science mission. This mission includes research in the natural sciences to provide a basis for new and improved energy technologies and for understanding and mitigating the environmental impacts of energy development and use. FERP also includes exploratory research in important new energy and environmental topics conducted under the Laboratory Directed Research and Development (LDRD) program. The scientific insights and breakthroughs achieved in FERP often become the underpinnings for projects that support DOE's applied research and development program offices.

Over the years, the basic earth sciences research program at Berkeley Lab has focused on three broad earth sciences problems:

1. Fundamental studies of chemical and mass transport in geologic media, with special reference to predictive modeling of multiphase, multicomponent, nonisothermal fluid flow in saturated and unsaturated fractured rocks

2. The development of new isotopic techniques for understanding the nature of a broad range of global processes— from the relatively short-term effects of natural fluid migration in the crust to longer-term (i.e., 10–20 thousand years) global climate variations

3. Fundamental studies in the propagation of seismic/acoustic and broadband electromagnetic waves through geologic media, with emphasis on new computational techniques for high-resolution imaging of near-surface and crustal structures (such as possible fracture flow paths) and for inferring the types of fluids present in pores and fractures

Results from these research endeavors have had a major impact on applied energy, carbon management/climate change, environmental, and radioactive waste management programs. Current research projects are briefly described here.

CHEMICAL AND MASS TRANSPORT INVESTIGATIONS

Current research in this area is focused on colloid transport in unsaturated porous media and rock fractures, chemical transport in structured porous media, unsaturated fast flow in fractured rock, and production and evaluation of coupled processes for CO_2 in aquifers. Our recent colloid research has been focused on quantifying the partitioning of surface-active colloids at the air-water interfaces. Much effort has been devoted to characterizing surface accumulations of colloids. We have recently developed a simple dynamic method to quantify colloid-surface excesses at air-water interfaces without requiring assumptions concerning the thickness of interfacial regions.

The studies of chemical transport in structured porous media have focused on Cr(VI) diffusion and reduction to Cr(III) within natural soil aggregates, to test the validity of our previously reported results from synthetic soil aggregates. Experiments were conducted on intact aggregates of Altamont clay. Work on unsaturated fast flow in fractured rock concerns water films on fracture surfaces under near-zero (negative) matric potentials and examines the possibility of fast, unsaturated flow under "tension." We showed that at matric potentials greater than that needed to saturate the rock matrix, transmissive water films can develop on fracture surfaces.

In the work on prediction and evaluation of coupled processes for CO_2 disposal in aquifers, the accuracy of published data and correlations for thermophysical properties of CO_2 (density, viscosity, enthalpy) is being evaluated for the range of pressure and temperature conditions of interest in aquifer disposal. Suitable correlations were implemented in our multipurpose simulator TOUGH2. Pre-existing models for CO_2 dissolution in aqueous fluids were enhanced by incorporating salinity and fugacity effects. Special techniques were developed for describing the movement of sharp CO_2-water interfaces during immiscible displacement of saline brines by CO_2.

ISOTOPE GEOCHEMISTRY

The Center for Isotope Geochemistry (CIG) is a state-of-the-art analytical facility established in 1988 to measure the concentrations and isotopic compositions of elements in rocks, minerals, and fluids in the earth's crust, atmosphere, and oceans. Fundamental research conducted at this center is directed at finding new ways to use isotopic information to study earth processes, such as long-term climate changes, and at predicting the chemical transport of mantle-derived or deep crustal fluids as they move through the crust.

One of the major problems being studied at CIG is how to estimate fluid-solid reaction rates in natural-groundwater higher-temperature geothermal conditions, particularly as these rates affect mineral dissolution and secondary mineral precipitation. ESD researchers are developing novel ways of estimating reaction rates by using isotopic tracers (primarily strontium, but also uranium and neodymium) to determine solid-fluid exchange rates in various natural situations. Scientists are able to derive the "reaction length," a parameter that depends on the ratio of isotope transport by diffusion and advection to the reaction rate. The ultimate objective is to understand the microscopic (as well as pore-scale and mesoscale) characteristics of natural systems that have been characterized in terms of "field scale" reaction-rate measures. An intermediate goal is to establish empirically the natural range of fluid-solid reaction rates.

ADVANCED COMPUTATION FOR EARTH IMAGING

The Center for Computational Seismology (CCS) was created in 1983 as the Berkeley Lab and UC Berkeley nucleus for seismic research related to data processing, advanced imaging, and visualization. In recent years, a great deal of cross-fertilization between seismologists and other geophysicists and hydrogeologists has developed within the division, resulting in collaborations on a wide variety of fundamental imaging problems. A primary thrust in this research has been to jointly develop seismic and electrical methods for understanding fluid flow and properties within the subsurface. In addition, fundamental studies on improved inversion and modeling of complex media in 3D are being carried out to analyze such effects as matrix heterogeneity fluid flow and anisotropy. Applications range from small-scale environmental problems to oil and gas reservoirs.

ROCK PHYSICS

A variety of rock and soil science experiments are being conducted through ESD's Geoscience Measurements Facility, which supports both field and laboratory work. In one new laboratory project, researchers are studying the compaction and fracturing of weakly cemented granular rocks. This study examines the effect of micromechanical properties of weak granular rock on macroscopic properties such as load-displacement response, ultimate strength, and failure mode. In a second study, a fundamental investigation of scattering and intrinsic attenuation of seismic waves in rock with heterogeneous distributions of fluids and gas is being conducted. This research represents a departure from past rock-physics studies on seismic attenuation, in that the emphasis here is not a detailed study of a specific attenuation mechanism, but rather to investigate theoretical and laboratory methods for obtaining separate estimates of scattering and intrinsic attenuation in rock with heterogeneous pore-fluid distributions.

FUNDING

Funding for research in the Fundamental and Exploratory Research Program comes from a variety of sources. These include (primarily) the U.S. Department of Energy, through the Director, Office of Science, Office of Basic Energy Sciences, Division of Chemical Sciences, Geosciences, and Biosciences; the Office of Biological and Environmental Research; the Assistant Secretary for Fossil Energy, Office of Natural Gas and Petroleum Technology, National Petroleum Technology Office, Natural Gas and Oil Technology Partnership; and the Office of Environmental Management Science Program. Funding is also provided by the Laboratory Directed Research and Development Program (LDRD) at Berkeley Lab.

U-Th/He Age Determinations on Volcanic Rocks: A New Tool for Quaternary Geochronology

Sarah M. Aciego, B. Mack Kennedy, John N. Christensen, Donald J. DePaolo, and Ian Hutcheon[1]
[1]Lawrence Livermore National Laboratory
Contact: Sarah M. Aciego, 510/486-4975, smaciego@lbl.gov

RESEARCH OBJECTIVES

Determining the age or time scale of events that have occurred within the past million years is still a challenge to geoscientists and an invaluable tool in evaluating hazards on the time scale of human life. Both radiocarbon and argon-argon (Ar-Ar) dating can be restricted due to a lack of appropriate phases or materials associated with the event. The uranium-thorium/helium (U-Th/He) system, which has been used successfully for thermochronology on zircon and apatite, has potential for dating young volcanic rocks. Our goal is to investigate the viability of applying the U-Th/He dating method to late Quaternary volcanic rocks containing relatively common minerals, such as garnet and olivine, that are not viable for Ar-Ar and radiocarbon dating.

APPROACH

The U-Th/He dating method is based on the radiogenic production of ^{4}He from the alpha decay of U and Th. An age is calculated for the accumulated ^{4}He/U-Th ratio measured in the sample. The accuracy of the age can be compromised by the high mobility of helium in most minerals, gain or loss of ^{4}He by alpha recoil, and isotopic disequilibrium in the U-Th-Pb decay chains. Therefore, to evaluate the viability of the method, we conducted a study of garnet phenocrysts from the 79 A.D. eruption of Vesuvius collected at the Villa of Poppea in Pompeii.

ACCOMPLISHMENTS

To thoroughly test the validity of this method for dating young samples, we had to address several issues: diffusive loss, trapped helium, loss or gain of ^{4}He from alpha recoil, and changing production of ^{4}He because of isotopic disequilibrium in the U and Th decay chains. Crushing and step-heating experiments were done to determine the amount of helium trapped and lost by diffusion. The distribution of U and Th was determined by ion microprobe techniques, and then applied to a simple model to determine loss and gain of helium by alpha recoil. Measurement of the isotopic ratios within the U-Th-Pb decay chains allowed us to correct the calculated age for radioactive equilibrium. Given these considerations, the resultant age of 1,866 ± 243 years indicates that the U-Th/He method is applicable to dating Holocene volcanic samples with accuracy and precision of ± 13% on samples with 20 ppm U.

SIGNIFICANCE OF FINDINGS

The calculated age of the Vesuvius lava validates the U-Th/He method for the dating of young volcanic systems. The age of the Vesuvius samples is extremely small compared to the 1.8 million year age range covered by the Quaternary epoch. Older samples should contain much larger amounts of radiogenic helium for the same amount of U and Th or similar amounts of helium for smaller concentrations of U and Th. The method can now be applied to a range of young lavas that contain fewer mineral phases and were previously not datable using existing Ar-Ar and radiocarbon techniques.

RELATED PUBLICATION

Aciego, S.M., B.M. Kennedy, D.J. DePaolo, J.N. Christensen, and I. Hutcheon, U-Th/He age of phenocrystic garnet from the 79 A.D. eruption of Mt. Vesuvius. Earth and Planetary Science Letters, 2003 (in press).

Renne, P.R., et al., Ar-40/Ar-39 dating into the historical realm, Calibration against Pliny the Younger. Science, 277, 1279-1280, 1997.
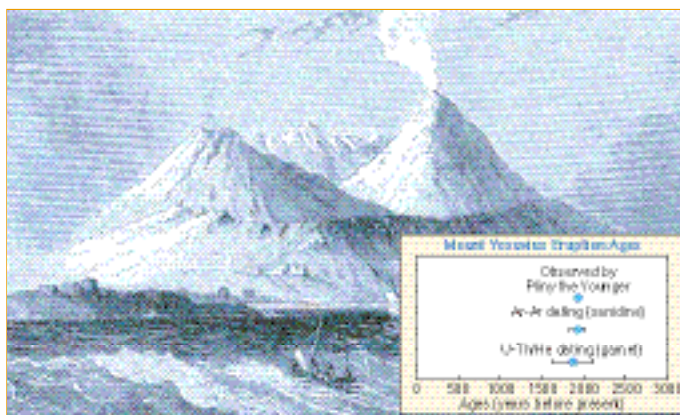
ACKNOWLEDGMENTS

Figure 1. Etching of 79 A.D. eruption of Mount Vesuvius as viewed from the sea. Inset is comparison of ages calculated using Ar-Ar dating (Renne et al., 1997) and U-Th/He dating with age determined by observations of Pliny the Younger.

KINETIC FRACTIONATION OF LITHIUM ISOTOPES BY DIFFUSION IN WATER

John N. Christensen, Frank Richter[1], and Ruslan Mendybaev[1]
[1]Department of Geophysical Sciences, University of Chicago
Contact: John N. Christensen, 510/486-6735, jnchristensen@lbl.gov

RESEARCH OBJECTIVES

The mass-dependent fractionation of stable isotopes can occur during a number of physical processes, only some of which are well understood theoretically and well investigated experimentally. In particular, the kinetic fractionation of isotopes during diffusion, though understood for gaseous systems, is not well characterized and understood for condensed systems such as liquid water or silicate melts. In the simple case of diffusion of a monatomic gaseous species in an isothermal gas, the ratio of the diffusivities for two isotopes of an element is proportional to the square root of the inverse ratio of the isotope masses. This arises from the equivalence in kinetic energy for molecules in an isothermal gas. In condensed systems such as silicate melts, this simple relationship does not appear to hold. We undertook experiments in aqueous solutions to better understand the phenomenon of kinetic fractionation during diffusion. Results could provide a signature for diffusion in geochemical systems, as well as add to fundamental understanding of the structure and behavior of ion complexes in aqueous solutions.
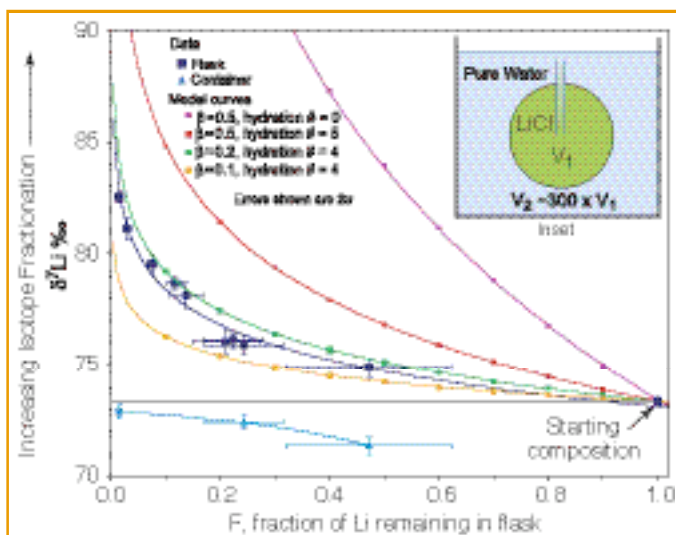

Figure 1. Plot of F, the fraction of Li remaining in the flask, vs. [7]Li, a measure of the Li isotopic composition. Large black squares = data for flasks, blue triangles = data for containers. Model curves are shown for different hydration numbers (# of waters in the hydration sphere) and exponential factors (=β). The inset shows the experimental setup, a flask of Li solution immersed and communicating with a larger volume of pure water.

APPROACH

The experimental setup consists of a 0.7 mL glass flask immersed in a larger (~300x) volume container (see inset, Figure 1). The flask is filled with a solution of the element of interest and communicates with the larger container via a thin tube. The experiments reported here used a ~700 ppm lithium chloride (LiCl) solution in the flask and high purity water in the surrounding container. Pairs of flasks and containers were set up and allowed to exchange for periods ranging from 31 days to 99 days. At the end of an experiment, we measured the concentrations of Li remaining in the flask and built up in the container. Lithium isotopic compositions ([7]Li/[6]Li ratios) were measured by multiple-collector ICP mass spectrometry (MC-ICPMS).

ACCOMPLISHMENTS

The results of nine experimental runs with durations ranging from 31 to 99 days are displayed in Figure 1, where F, the fraction of the original Li remaining in the bulb, is plotted against δ[7]Li, a measure of Li isotopic composition. The longest duration experiment left only 1.5% of the original amount of Li in the flask, the balance having diffused into the container volume. As F decreases and Li diffuses from the flask, the isotopic composition of the Li in the flask is fractionated, with more of the heavier [7]Li left in the flask than the lighter [6]Li. This demonstrates that kinetic fractionation of Li isotopes does occur, in contrast to similar experiments involving magnesium that failed to resolve a fractionation effect.

SIGNIFICANCE OF FINDINGS

Though fractionation was observed, it was not as great as would be predicted by the theory for gaseous diffusion. A portion of the discrepancy may result from Li^{+} diffusing as a hydrated complex, diluting the [6]Li-[7]Li mass difference. Models and observations suggest that a sphere of four to six water molecules surrounds Li^{+} ions. But for an exponent of 0.5, as for a gas, it would require a sphere of 11 waters, an improbable number. If the hydration sphere consists of four waters, then an exponential factor of ~0.2 reproduces the data. This may reflect the inelastic nature of interactions between water molecules and the Li^{+} hydrated complex. Further experiments are being conducted to better understand and independently constrain the exponential factor and the hydration number.

ACKNOWLEDGMENTS

FILM FLOW ALONG TUNNEL WALLS

Teamrat A. Ghezzehei and Stefan Finsterle

Contact: Teamrat A. Ghezzehei, 510/486-5688, taghezzehei@lbl.gov

RESEARCH OBJECTIVES

Dripping of liquid water into tunnels or caves affects natural processes (such as formation of speleothems) and is important to engineering applications (such as mining and geologic disposal of nuclear wastes). Current computer models of these processes assume that liquid water drips immediately after entering the tunnel. In contrast, recent field observations showed that film flow and wetting of tunnel walls result in a temporal and spatial lag between liquid emergence and subsequent dripping. The objective of this research is to assess the impact on seepage of film flow along rough tunnel walls and provide a framework for realistic modeling of seepage and evaporation.

APPROACH

In this research, conceptual models are developed by capitalizing on recent advances in our understanding and modeling of (1) unsaturated flow near and around tunnels, (2) characterization of unsaturated flow on rough surfaces, and (3) dripping from pendant rivulets. To provide better insight into these hitherto poorly understood phenomena, the research favors analytical models that use simplified geometries and flow conditions.

ACCOMPLISHMENTS

The conceptual model developed thus far is schematically described in Figure 1. Liquid water enters subsurface tunnels at regions where the near-ceiling pores or fractures are fully saturated. Subsequently, the rough tunnel walls intercept the liquid, and film flow occurs, mediated by the *capillary roughness,* which is generally on the order of one millimeter. Flow along the unsaturated wall is driven by capillary and gravitational gradients, as described by the Buckingham-Darcy law. In the unsaturated portions of the tunnel wall, relatively strong capillary adhesion prevents dripping. Dripping occurs at any location on the ceiling where sufficient positive pressures develop with aerial extent equivalent to the base area of a pendant drop. To facilitate derivation of an analytical solution, we developed a one-dimensional steady-state model for a cylindrical tunnel, as shown in the right panel of Figure 1.

SIGNIFICANCE OF FINDINGS

Typical capillary pressure (ψ) profiles for several tunnel sizes are shown in Figure 1. Generally, the wetness of the crown region increases with tunnel size because of reduced gravitational forces that are insufficient to drive the liquid away. Consequently, larger tunnels are more prone to dripping. The variable wetness of tunnel walls can be used for physically based estimation of evaporation losses into the tunnel air.

RELATED PUBLICATION

Ghezzehei, T.A., and S. Finsterle, Film flow on tunnel walls and its role in decreasing seepage. Vadose Zone Journal, 2003 (submitted).
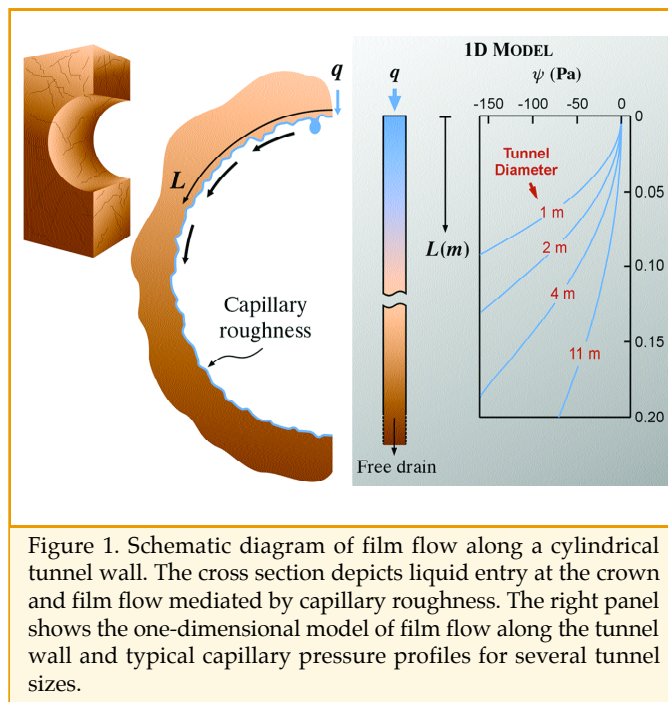
ACKNOWLEDGMENTS

Figure 1. Schematic diagram of film flow along a cylindrical tunnel wall. The cross section depicts liquid entry at the crown and film flow mediated by capillary roughness. The right panel shows the one-dimensional model of film flow along the tunnel wall and typical capillary pressure profiles for several tunnel sizes.

AIR-DERIVED NOBLE GASES IN SEDIMENTS: IMPLICATIONS FOR BASIN-SCALE HYDROGEOLOGY

B. Mack Kennedy, Tom Torgersen[1], and Matthijs C. van Soest
[1]Department of Marine Sciences, University of Connecticut
Contact: B. Mack Kennedy, 510/486-6451, bmkennedy@lbl.gov

RESEARCH OBJECTIVES

The goal of this project is to isolate and identify the various air-derived noble gas components in sediments, particularly (but not exclusively) those sediments associated with hydrocarbon systems. This project is designed to address how noble gas elemental patterns are acquired and retained in rocks and minerals and how they are transferred to the fluid phases in which they have been measured.

APPROACH

Laboratory and theoretical studies are carried out to (1) identify and isolate the carrier phases of the various air-derived noble gas components in sedimentary rocks and minerals, (2) investigate the process(es) responsible for acquisition and subsequent trapping of the components in their sedimentary carrier phases, and (3) evaluate the mechanisms that release these noble gas components to the ambient hydrological system under temperatures and pressures encountered in natural basin processes.

ACCOMPLISHMENTS

We have examined adsorption and diffusion-controlled fractionation of noble gases as an explanation for the absolute and relative abundances observed in sedimentary rocks. The model uses diffusive filling and emptying of (1) angstrom-scale half spaces and (2) a system of labyrinths-with-constrictions on the order of the diffusing species' atomic diameter (Figure 1a). Since physical properties of the noble gases are strong functions of atomic mass, the individual diffusion coefficients, adsorption coefficients, and atomic diameters combine to enhance the transport of neon (Ne) while impeding xenon (Xe) (Figure 1b).

SIGNIFICANCE OF FINDINGS

The model results compare favorably with literature data for noble gas concentrations and relative abundances in terrestrial rocks. It is generally assumed that the source for all atmospheric noble gases in subsurface fluids is air-saturated water. Evidence for water-derived noble gases in hydrocarbon systems is extensive and provides strong support that water plays an important role in hydrocarbon systems. However, excesses of atmospheric xenon and neon recently identified in hydrocarbon systems may be derived from the source and reservoir rocks associated with the system (Torgersen and Kennedy, 1999; Kennedy et al., 2002). If so, future noble gas studies of fluid sources and flow will have to consider sediments as potential sources for atmospheric noble gases, which up till now have been mostly ignored.

RELATED PUBLICATIONS

Torgersen, T., and B.M. Kennedy., Air-Xe enrichments in Elk Hills oil field gases: Role of water in migration and storage. Earth Planet. Sci. Lett., 167, 239–253, 1999.

Kennedy, B.M., T. Torgersen, and M.C. van Soest, Multiple atmospheric noble gas components in hydrocarbon reservoirs: A study of the Northwest Shelf, Delaware Basin, SE New Mexico. Geochim Cosmochim Acta., 66, 2807–2822, 2002.
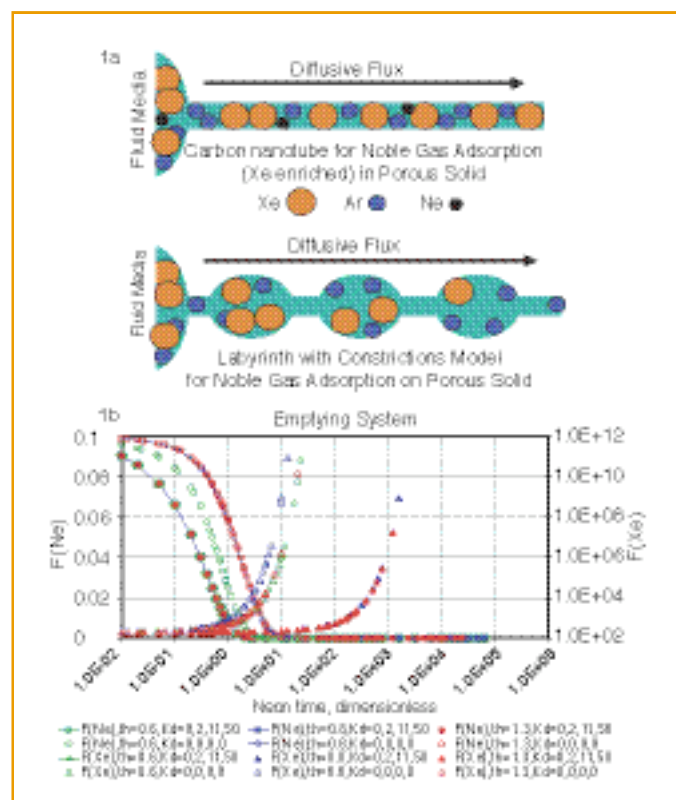
ACKNOWLEDGMENTS

Figure 1: (a) Cartoons depicting the diffusive flow of noble gases through an angstrom-scale half-space (carbon nanotube) and a system of labyrinths and constrictions; (b) relative enrichment/depletion of noble gases as a function of time and effective diffusivities (Kd) and throat constriction diameters (th). The F(Ne,Xe) values are the abundances of Ne and Xe with respect to Ar, normalized to the Ne,Xe/Ar ratios in air.

Noble Gas Isotope Studies of Geothermal Systems

B. Mack Kennedy and Matthijs C. van Soest
Contact: B. Mack Kennedy, 510/486-6451, bmkennedy@lbl.gov

RESEARCH OBJECTIVES

This project develops isotope tracers for identifying fluid and heat sources and studying fluid processes in geothermal systems. Recently, we have concentrated on identifying geochemical and/or isotopic signals that can be used to locate geothermal systems in regions lacking recent volcanic activity and surface manifestations of deep hot fluids.

APPROACH

Fluids within the earth's crust contain noble gases (helium [He], neon [Ne], argon [Ar], krypton [Kr], and xenon [Xe]) from a variety of sources, each characterized by a unique composition, and therefore contributions from different sources can be easily identified. For instance, geothermal fluids that acquire heat from active magma systems are strongly enriched in ^{3}He, with ^{3}He/^{4}He ratios up to 9 times the ratio in air (R/Ra ~ 9); those that acquire heat from the natural thermal gradient are depleted in ^{3}He (R/Ra ~ 0.02). This vast difference provides a sensitive quantitative measure of fluid and heat source driving a geothermal system and fluid mixing within the system.

ACCOMPLISHMENTS

The Dixie Valley Geothermal Field, Nevada, is considered a classic nonmagmatic geothermal system that acquires heat by deep fluid circulation. Similar systems occur throughout the Basin and Range Province of northern Nevada. Fluids sampled throughout Dixie Valley (Figure 1a) have a range in helium isotopic compositions (~0.3–0.8 Ra). The highest values (0.7–0.8 Ra), found in fluids produced from the Dixie Valley Geothermal Field, suggest that the natural thermal gradient provides ~85–90% of the reservoir heat. Co-variations between He isotopic composition and abundances (Figure 1b) require mixing of two fluids, and also require that all of the sampled features (except Well 66-21) contain a fluid component indistinguishable from that produced from the geothermal field.

SIGNIFICANCE OF FINDINGS

The observation of a common deep fluid throughout Dixie Valley suggests the presence of a larger exploitable geothermal resource than presently under production. This study also demonstrates the utility of noble gas isotopes for finding and evaluating the extent of hidden geothermal systems.

RELATED PUBLICATIONS

Kennedy, B.M., M.C. van Soest, and S. Johnson, Helium isotopes in Dixie Valley wells, springs, and fumaroles: Heat and fluid sources; regional trends. Geothermics, 2003 (submitted).

Kennedy, B.M., T.P. Fischer, and D.L. Shuster, Heat and helium in geothermal systems. Proceedings, 25th Workshop on Geothermal Reservoir Engineering, Stanford Geothermal Program Report SGP-TR-165, pp. 167–173, 2000.
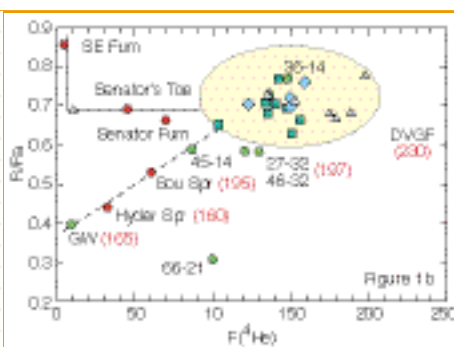
ACKNOWLEDGMENTS

Figure 1a: Map showing the location of Dixie Valley wells, springs, fumaroles, and the Dixie Valley Geothermal Field. Features identified by letters (see Legend) were sampled for noble gas isotope analyses.

Figure 1b: Helium isotopic compositions (R/Ra) for the Dixie Valley samples are plotted as a function of the 4He/36Ar ratio (normalized to the ratio in air). The F(4He) values reflect the degree of helium enrichment relative to that expected for young meteoric waters [F(4He)~ 0.2]. The composition of Dixie Valley geothermal production wells plot within the ellipse. The dotted line emanating from the ellipse portrays the trajectory expected for either boiling (e.g., Senator's Toe and Fumarole) or air contamination (SE Fumarole). The dashed line depicts two fluids mixing. Numbers in parentheses are calculated chemical geothermometer temperatures.

Synthesis, Characterization, and Reactivity of Nanoparticulate Goethite

Christopher S. Kim, Jill F. Banfield, and Glenn A. Waychunas

Contact: Christopher S. Kim, 510/486-7709, cskim@lbl.gov

RESEARCH OBJECTIVES

Nanoparticles feature high surface areas, a tendency to remain in suspension, and differences in their chemical/physical properties relative to bulk phases. As a result, the reactivity of nanoparticles to metal contaminants (e.g., As, Cu, Hg, Zn) may be greatly enhanced in inverse proportion to their size. The objectives of this research are to study the formation, growth, and reactivity of nanoparticulate goethite (α-FeOOH), one of the most common mineral phases in the environment and one of the most reactive in terms of metal-contaminant uptake.

APPROACH

Our approach involves the synthesis and characterization of nanoparticulate goethite over a range of sizes (from 10 to 100 nm). Studies of goethite nanoparticle growth over time are then paired with metal uptake studies and analysis of metal speciation at the mineral-water interface to understand any changes in reactivity as a function of size. Transmission electron microscopy (TEM), surface area analysis, x-ray diffraction (XRD), and dynamic light scattering (DLS) are used to characterize the differently sized batches of nanoscale goethite and determine their size, morphology, surface area, and size distribution. The growth and structure of the nanoparticles are investigated through small- and wide-angle x-ray scattering (SAXS/WAXS) spectroscopy, while metal uptake is studied using batch sorption experiments paired with inductively coupled plasma-atomic emission spectrometry (ICP-AES) and extended x-ray absorption fine structure (EXAFS) spectroscopy.

ACCOMPLISHMENTS

We have synthesized goethite over a range of 10–80 nm in diameter (surface areas >250 m²/g), using a microwave annealing process and aging at 90°C. The size distribution of the nanogoethite has been characterized with DLS and TEM. Analyzing aged samples with DLS shows that the nanogoethite exhibits two stages of growth (Figure 1): relatively rapid growth from 0 to 4 days (10–58 nm) and much slower growth from 4 to 33 days (58–78 nm). This may represent initial evidence of (oriented) aggregation as a mechanism for nanoparticle growth, in agreement with recent studies indicating that growth through aggregation dominates over growth from solution. This distinction is important in predicting the eventual fate/sequestration of metals that may sorb to nanoparticles during their growth.

The SAXS/WAXS spectroscopy work has focused on the *in situ* growth of nanoparticulate goethite suspensions at 90°C.

Batch uptake experiments and corresponding EXAFS analysis have shown differences in the mode of metal speciation between 10 nm and 73 nm batches of goethite, indicating that there is a particle-size dependency on the method of metal sorption, perhaps caused by varying densities or proportions of sorption sites as a function of size.

SIGNIFICANCE OF FINDINGS

This work has important, fundamental implications for our understanding of how the properties of nanoscale materials, including reactivity to metals, may deviate with decreasing particle size. In addition, this research has potential applications in remediation of abandoned mines or industrially polluted regions, where high-surface-area, hypersorbent phases such as nanoparticulate goethite may assist in the cleanup of heavy metals.
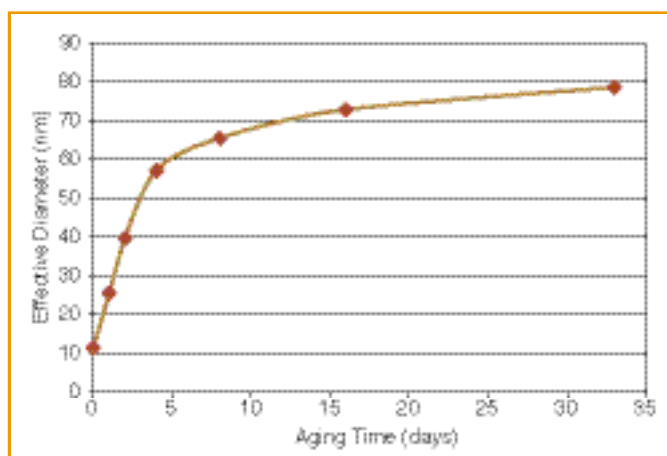

Figure 1. Dynamic light scattering (DLS) measurements tracking the growth of goethite nanoparticles as a function of aging time at 90°C.

RELATED PUBLICATION

Waychunas, G.A., Structure, aggregation, and characterization of nanoparticles. In Nanoparticles and the Environment (J.F. Banfield and A. Navrotsky, editors), Mineralogical Society of America, 2001.

ACKNOWLEDGMENTS

FAULT ZONE IMAGING USING GUIDED WAVES

Valeri Korneev and Robert Nadeau
Contact: Valeri Korneev, 510/486-7214, vakorneev@lbl.gov

RESEARCH OBJECTIVES

The main goal of this project is to develop new seismic image processing technologies. These technologies will improve the quality and resolution of seismic images for complex media, as well as increase our knowledge of the physical processes in rocks.

APPROACH

A significant part of the project involves furthering our understanding of seismic wave propagation in an active fault zone. Our method involves attributing specific features of recorded seismic waves to the structural and physical properties of the fault, which allow extraction of more detailed information from the data. Analysis and interpretation of the data enable extensive numerical modeling of seismic wave propagation in the fault zones. We use microearthquake data from Parkfield, California (located on the San Andreas fault) to apply the new forward modeling techniques we have developed for use on a crustal scale. These techniques are complemented by an innovative guided-wave tomography inversion scheme to obtain high-resolution images of the fault zone core.

Numerical modeling and a number of field observations have indicated the usefulness of propagating fault zone guided waves (FZGW) at Parkfield, which has a 20 to 40% low-velocity fault zone 100 to 200 m wide.

ACCOMPLISHMENTS

Using amplitude guided-wave tomographic inversion, we obtained a unique image (Figure 1) of the inner structure of the San Andreas fault zone, with resolution exceeding travel-time P- and S- wave tomography by a factor of ten. The results show clearly that FZGW are most effectively generated within a well-defined region of the fault zone. This region plunges to the northwest through an area of extremely high seismicity, separating locked and slipping sections of the fault (as determined from both geodesy and microearthquake recurrence rates). We interpret this localized region of FZGW generation to be the northwest edge of the M6 asperity at Parkfield, the low attenuation most likely resulting from dewatering by fracture closure and/or fault-normal compression. Changes in fracture orientation, caused by a complex stress field in the boundary of creeping and locked zones of the fault, are also likely causes of the low attenuation.

SIGNIFICANCE OF FINDINGS

The obtained images indicate a high connectivity between various spatially dependent parameters (such as slip rate, stress change, and wave propagation velocities), which suggests their common origin. This study also shows that FZGW can be used for amplitude tomographic inversion, giving high-resolution, robust images of the narrow low-velocity layers (faults). FZGW-generated images contain several significant features of the fault zone—the region of shallow velocity change in the Vibroseis monitoring, high seismicity, the largest earthquakes and associated high slip rate, the 1966 M6 hypocenter, and the transition from locked to creeping behavior. These results, and specifically the content and quality of the produced images, reinforce the importance of guided waves for fault zone studies.

RELATED PUBLICATION

Korneev, V.A., R.M. Nadeau, and T.V. McEvilly, Seismological studies at Parkfield IX: Fault zone imaging using guided wave attenuation. Bulletin of Seismological Society of America, 2003 (in press).
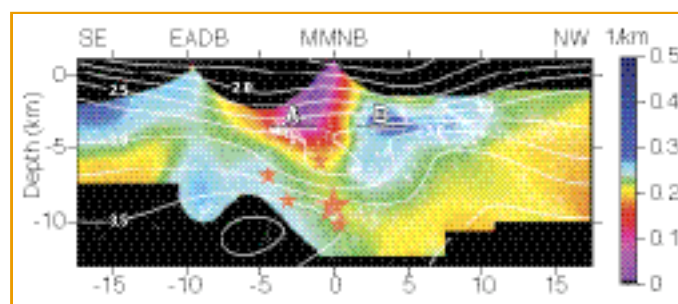
ACKNOWLEDGMENTS

Figure 1. In-fault attenuation-coefficient image of the FZGW tomographic reconstruction, showing the northwest-plunging region of inferred strong fault zone guided-wave generation, Vs contours, 1987–1998 seismicity (small red stars for M>4 events), and the 1966 M6 hypocenter

JOINT INVERSION FOR MAPPING SUBSURFACE HYDROLOGICAL PARAMETERS

Ki Ha Lee and Hung-Wen Tseng
Contact: Ki Ha Lee, 510/486-7468, khlee@lbl.gov

RESEARCH OBJECTIVES

One of the main objectives of geophysical inversion is to describe various subsurface processes involving fluid flow. Hydrological properties such as fluid electrical conductivity and rock porosity cannot be directly obtained with conventional inversion techniques. The electromagnetic (EM) field propagating in the subsurface is a function of bulk conductivity, which in turn may be empirically related to porosity, pore-fluid conductivity, saturation, and occasionally the temperature. Similarly, the amplitude, phase, and velocity of seismic waves depend on several factors (such as porosity, density, elastic constants, temperature, and pressure). The objective of this study was to develop methodologies for directly mapping hydrological parameters using joint analysis of different geophysical data, along with the empirical relationships between geophysical and hydrological parameters.

APPROACH

To assess the feasibility of deriving hydrological properties directly, we introduced a joint-inversion technique using electromagnetic (EM) and seismic travel-time data (Tseng and Lee, 2001). Because of the limited capability inherent to the inversion techniques used, we decided to investigate advanced inversion schemes for the improved joint inversion. Most of the EM inversion studies in the literature involve full waveform, but there is a lack of similar studies in the seismic area. Full-waveform inversion of seismic data is difficult, partly because of the lack of precise knowledge about the source. Since currently available approaches involve some form of source approximation, inversion results are subject to the quality and choice of the source information used.

ACCOMPLISHMENTS

A new full-waveform inversion scheme has been developed in this research program, exploiting the useful property of the normalized wavefield. A gather of seismic traces was first Fourier-transformed into the frequency domain, and a normalized wavefield was obtained for each trace in the frequency domain. Normalization was done with respect to the frequency response of a reference trace selected from the gather. The source spectrum was eliminated during the normalization procedure. With its source spectrum eliminated, the normalized wavefield allowed us to construct an inversion algorithm without the source information. The inversion algorithm minimized misfits between the measured normalized wavefield and the numerically computed normalized wavefield.

The validity of the scheme has been successfully demonstrated using a simple 2-D synthetic model (Lee and Kim, 2003).

SIGNIFICANCE OF FINDINGS

Normalized wavefields depend, for a given source, only on the subsurface model and the position of the source, and are independent of the source spectrum by construction. The significance of this is that full-waveform inversion of seismic data can be achieved without the source information. With the new method, potential inversion errors caused by source estimation (required by conventional full-waveform inversion methods) can be eliminated.

RELATED PUBLICATIONS

Lee, K.H., and H.J. Kim, Source-independent full waveform inversion of seismic data. Geophysics (in press), published electronically on May 20, 2003; Berkeley Lab Report LBNL-49934.

Tseng, H.-W., and K.H. Lee, Joint inversion for mapping subsurface hydrological parameters. Expanded Abstracts, SEG International Exposition and 70th Annual Meeting, San Antonio, Texas, pp. 1341–1344, September 9–14, 2001.

ACKNOWLEDGMENTS

Use of ^{234}U/^{238}U Ratios to Measure *In Situ* Weathering Rates in the Hanford Vadose Zone

Katharine Maher, Donald J. DePaolo, and John N. Christensen
Contact: Katharine Maher, 510/642-9524, katem@eps.berkeley.edu

RESEARCH OBJECTIVES

Weathering rates of subsurface soil and rocks are difficult to quantify because of the difficulties in assessing the amount of reactive surface area and the thermodynamic potentials driving the chemical reactions. Mineral dissolution rates measured in the laboratory typically predict rates that are 2 to 4 orders of magnitude faster than estimates based on field measurements (White et al., 1996). Few field measurements are available, and most of those are on silicate soils. Almost no field measurements exist for deep vadose zone materials or for rocks in the saturated zone.

The uranium-series (U-series) isotope system can be used to measure reaction rates in aquifers and thick vadose zone environments. This approach is based on α-recoil of ^{234}Th atoms across grain boundaries, which enriches the pore fluid in ^{234}U. Dissolution of the solid phase releases mainly ^{238}U to the pore fluid, so that the ^{234}U/^{238}U ratio of the pore fluid is a measure of the local ratio of the dissolution uranium flux to the α-recoil flux (Tricca et al., 2001; DePaolo et al., 2003 submitted). The *in situ* reaction rate can be calculated from measurements of the ^{234}U/^{238}U isotopic ratio of interstitial fluids and solid phases, if the α- recoil flux can be estimated independently.

APPROACH

Uranium isotopes were measured for bulk sediment, sediment size fractions, pore fluids, the exchangeable fraction, and selected mineral phases of a 70 m vadose zone core at the Hanford Site, Washington, to estimate the mineral weathering rates and understand uranium distributions in the vadose zone. These measurements were performed using a Micromass IsoProbe multicollector ICP-MS at the Center for Isotope Geochemistry. A reactive transport model, aimed at comparing the U-series kinetics to those predicted by a multicomponent thermodynamic model, is being constructed to further evaluate the results.

ACCOMPLISHMENTS

The measured ^{234}U/^{238}U ratios for the vadose zone core yield weathering rates that are in general agreement with estimates based on other methods: approximately $10^{-6.4}$ yr^{-1} (Figure 1). These are the first measurements of uranium isotope compositions of the vadose zone pore waters and solid phases, and the first attempt to use these measurements to estimate weathering rates in the vadose zone.

SIGNIFICANCE OF FINDINGS

This study is the first to quantify reaction kinetics in the vadose zone. Perhaps the most significant contribution of this work is the development of an *in situ* method for determining

precipitation/dissolution rates that, when coupled with other geochemical data, may help to decipher the mechanisms that control weathering in natural systems.

RELATED PUBLICATIONS

DePaolo et al., Rate of diagenetic reactions in deep-sea sediment: *In situ* measurement using ^{234}U/^{238}U of pore fluids. Geochim. Cosmochim. Acta., 2003 (submitted).

Maher, K., D.J. DePaolo, M.E. Conrad, and R.J. Serne, Vadose zone infiltration rate at Hanford, Washington, inferred from Sr isotope measurements. Water Resour. Res., 39(8), 1204, 2003.

Tricca, A., G.J. Wasserburg, D. Porcelli, and M. Baskaran, The transport of U- and Th- series nuclides in a sandy unconfined aquifer. Geochim. Cosmochim. Acta, 65, 1187–1210, 2001.

White, A.F., A.E. Blum, M.S. Schulz, T.D. Bullen, J.W. Harden, and M.L. Peterson, Chemical weathering of a soil chronosequence on granitic alluvium 1. Reaction rates based on changes in soil mineralogy. Geochim. Cosmochim. Acta, 60, 2533–2550, 1996.
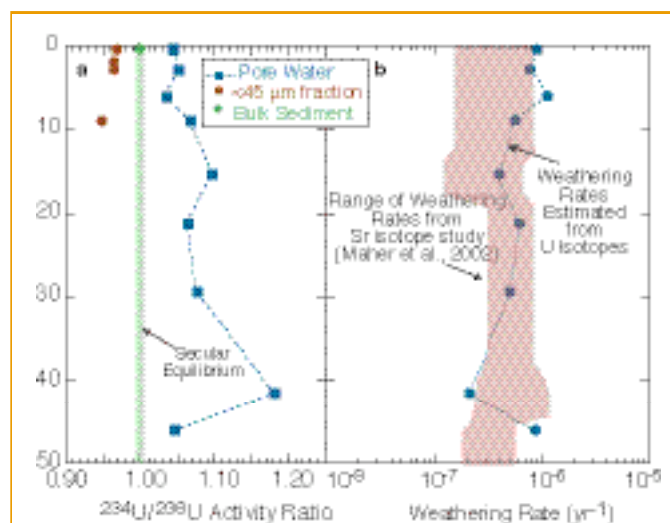
ACKNOWLEDGMENTS

Figure 1. (a) U isotope data from the 299-W22-48 core, Hanford, Washington. (b) Comparison of estimated weathering rates derived from Sr and U isotope studies.

DETECTION AND IDENTIFICATION OF UNEXPLODED ORDNANCE

Frank Morrison, Alex Becker, Erika Gasperikova, and Torquil Smith

Contact: Erika Gasperikova, 510/486-4930, egasperikova@lbl.gov

RESEARCH OBJECTIVES

A recent Task Force Report lists some 1,500 sites comprising approximately 15 million acres that potentially contain unexploded ordnance (UXO). In practice, the major costs in cleanup are excavation and removal, but at present, 90% of the objects detected are non-UXO, and 75% of the cost of excavation is for these non-UXO objects. Existing systems can detect metallic objects in the ground, but cannot discriminate between the generally cylindrical and symmetric intact UXO and the scraps or fragments of exploded UXO that are harmless (Figure 1). It is the objective of this research to design and fabricate an optimum active electromagnetic (AEM) system that can extract from the measurements the best possible estimates of the location, size, shape, and metal content of a buried metallic object—in the presence of interfering responses from the ground and non-UXO metallic objects.

APPROACH

These objectives are being realized through simulators: numerical models of the electromagnetic response, produced by an arbitrary target in the ground, to an arbitrary configuration of transmitters and receivers. The simulators are then used for the forward calculations required in inverse solutions for (a) the depth, size, and aspect ratio of a target and (b) the configuration of the transmitters and receivers to optimize the calculations in (a).

ACCOMPLISHMENTS

We have found that the depth, size, and principal moments (any target can be represented by three orthogonal principal dipole moments) can be derived from the response of a system consisting of three orthogonal transmitters and five sensitive induction-coil sensors mounted within a $1\,m \times 1\,m$ frame. Because of these findings, the project emphasis has shifted to making magnetic field sensors and instrumentation that can achieve measurement bandwidths (or time windows) that meet the specifications of the simulations. Since optimum determination of depth and orientation requires multiple-point sensors (arrays of compact sensors), we have developed small induction sensors to replace the large open-loop sensors currently used in all AEM systems.
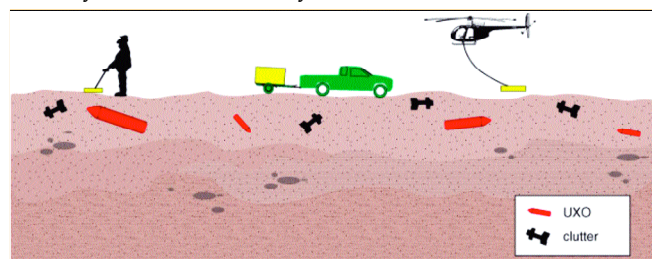

Figure 1. Conceptual representation of UXO in presence of clutter and geological noise

SIGNIFICANCE OF FINDINGS

We have designed a new generation of multisensor electromagnetic systems that can significantly extend the depth of UXO detection and, more importantly, determine key parameters of the object that will differentiate it from harmless scrap metal.

ACKNOWLEDGMENTS

SEISMIC WAVE SCATTERING BY HETERGENEOUS FRACTURES AND FAULTS

Seiji Nakagawa, Aoife C. Toomey, and Larry R. Myer
Contact: Seiji Nakagawa, 510/486-7894, snakagawa@lbl.gov

RESEARCH OBJECTIVES

The conventional seismic displacement discontinuity (SDD) model for seismic wave scattering by single fractures and faults assumes a linear relationship between the wave-introduced, small relative displacement and the stress across a fracture. This relationship is represented by a material parameter called fracture compliance. Theoretical studies based upon the SDD model are usually limited to, or assume, fractures with a homogeneous distribution of fracture compliance on the fracture plane. Naturally occurring fractures and faults are, however, heterogeneous, with the microscale properties varying along the fracture plane. This variation gives rise to fracture compliance that is spatially heterogeneous and, possibly, auto-correlated. Since the heterogeneity of a fracture has a great impact on the hydraulic and mechanical properties of the fracture, understanding the effect of heterogeneity on the scattering of elastic waves can provide valuable tools for geophysical and nondestructive characterization of fracture properties.

APPROACH

The dynamic behavior of a real fracture and a fault can be modeled using an interface with a heterogeneous distribution of compliance, measured locally at some length scale much smaller than the seismic (elastic-wave) wavelengths. Analytical and numerical techniques to examine elastic-wave scattering by heterogeneous fractures and faults can be developed based on these "local" SDD boundary conditions and the plane-wave theory. This is achieved by simply applying a spatial Fourier transform to the conventional SDD conditions with the "local" fracture compliance. For this reason, this method is called the wavenumber-domain seismic-displacement-discontinuity (wd-SDD) method.

ACCOMPLISHMENTS

An analytical model of the wd-SDD method was developed, and a numerical algorithm was written to simulate elastic-wave scattering by heterogeneous fractures and faults. The heterogeneity is quantitatively represented as a spatially correlated, random distribution of the fracture compliance on a fracture or fault plane. Some of the advantages of this method are that (1) wave scattering for a wide range of frequencies can be examined, (2) all mode-converted waves can be modeled (Figure 1), and (3) only a small computer is needed for the numerical simulations.

SIGNIFICANCE OF FINDINGS

Using the developed method, we examined the scattering-induced, frequency-dependent behavior of average fracture compliance determined from the scattered waves measured in the far field. Our results showed that, for a spatially correlated, heterogeneous fracture-compliance distribution with a finite correlation length, the average compliance increases as a function of frequency at low frequencies, and then decreases at high frequencies. The transition frequency between the low and high frequency regimes can be related to the correlation length of the distribution. In contrast, for a self-affine (fractal) compliance distribution that does not have characteristic length scale, the numerical simulations show little or no peak in the compliance spectra. Also, these frequency-dependent compliances have a complex value, which can be misinterpreted as the viscoelastic property of the fracture.

RELATED PUBLICATION

Nakagawa, S., K.T. Nihei, and L.R. Myer, Elastic wave scattering of a fracture with non-uniform stiffness distribution. EOS Trans., AGU, 83(47), Fall Meet. Suppl., Abstract S61B-1141, 2002.
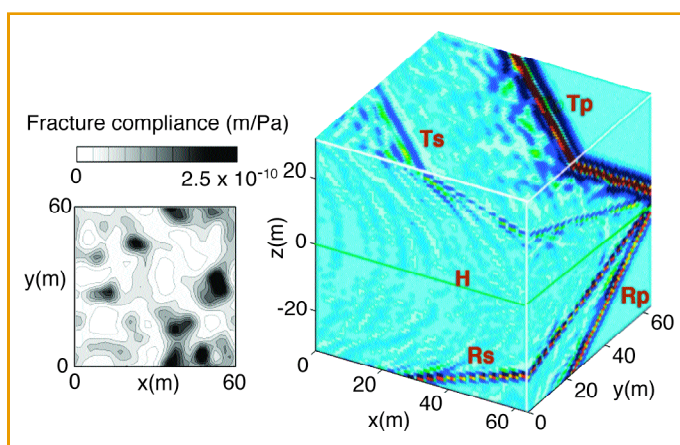
ACKNOWLEDGMENTS

Figure 1. A computed three-dimensional snapshot (z-direction displacements) of plane elastic waves scattered by a fracture (shown as a green line at the center of the cube) with a heterogeneous compliance distribution. The propagation direction of the incident wave is (x, y, z)=(1,1,1). The symbols in the plot indicate Tp, transmitted compressional wave; Rp, reflected compressional wave; Ts, transmitted shear wave; Rs, reflected shear wave; and H, fracture head waves.

IMAGING ATTENUATION IN ROCK WITH HETEROGENEOUS MULTIPHASE FLUIDS

Kurt T. Nihei, S. Nakagawa, and T. Watanabe

Contact: Kurt T. Nihei, 510/486-5349, ktnihei@lbl.gov

RESEARCH OBJECTIVES

At the center of this project is a fundamental investigation of scattering and intrinsic attenuation of seismic waves in rock with heterogeneous distributions of fluids and gas. This research represents a departure from past rock-physics studies on seismic attenuation, in that the emphasis here is not on a detailed study of a specific attenuation mechanism. Rather, the emphasis is on investigating theoretical and laboratory methods for obtaining separate estimates of scattering and intrinsic attenuation in rock with heterogeneous pore-fluid distributions. We anticipate that methods for obtaining separate estimates of intrinsic and scattering attenuation may lead to higher-resolution methods for monitoring the movement of fluids in the subsurface.

APPROACH

During the first two years of this project, we have adopted a deterministic approach to the problem of attenuation imaging. The approach is to use full-waveform viscoelastic nonlinear inversion to image the frequency-dependent viscoelastic properties of the subsurface. The complex moduli determined from this inversion provide estimates of the frequency-dependent bulk and shear moduli and the P- and S-wave intrinsic attenuation. In principle, if the finite-difference modeling code used in the full-waveform inversion scheme correctly simulates wave propagation in a heterogeneous, viscoelastic medium, and the source-receiver coverage around the medium being probed is adequate, then the apparent attenuation caused by scattering off heterogeneities is removed in the inversion process. The attenuation estimated from the inverted complex moduli will be the intrinsic attenuation. However, in practice, it is expected that cumulative scattering off subwavelength heterogeneities (e.g., layering) may also effectively remove energy from the dominant arrivals. This research will use numerical modeling with heterogeneity to investigate these issues.

ACCOMPLISHMENTS

One key component of full-waveform viscoelastic imaging is its efficient numerical algorithm for computing the seismic response at the receiver locations for multiple sources. We have found that a faster finite-difference solution for time harmonic problems can be computed with an explicit (i.e., time-domain) method rather than an iterative implicit (i.e., frequency-domain) method. In this time-domain approach to frequency-domain modeling, a time-domain finite-difference code is run with harmonic waves out to steady state (Figure 1). The magnitude and phase at each location (x,z) are extracted from the time harmonic data using a phase-sensitive detection (PSD) algorithm. Tests performed using this algorithm demonstrate that it requires a simple summation over several cycles to obtain accurate magnitude and phase estimates. Tests have also shown that the algorithm works when multiple frequencies are present in the wavefield.

SIGNIFICANCE OF FINDINGS

Based on these results, a 2-D viscoelastic, anisotropic, frequency-domain, full-waveform inversion code is being built around a 2-D viscoelastic, anistropic, time-domain, staggered-grid finite-difference code. We anticipate that this code will be significantly faster than, and capable of solving larger problems than, current viscoelastic frequency-domain inversion codes that utilize frequency-domain forward-modeling routines. We plan on completing and testing this inversion code later in 2003.

RELATED PUBLICATION

Watanabe, T., K.T. Nihei, S. Nakagawa, and L.R. Myer, Imaging of crosshole laboratory data using visco-acoustic waveform inversion and reverse-time imaging. Expanded Abstracts, 72nd Annual Meeting of the Society of Exploration Geophysics, Salt Lake City, Utah, pp. 870–873, 2002.

ACKNOWLEDGMENTS

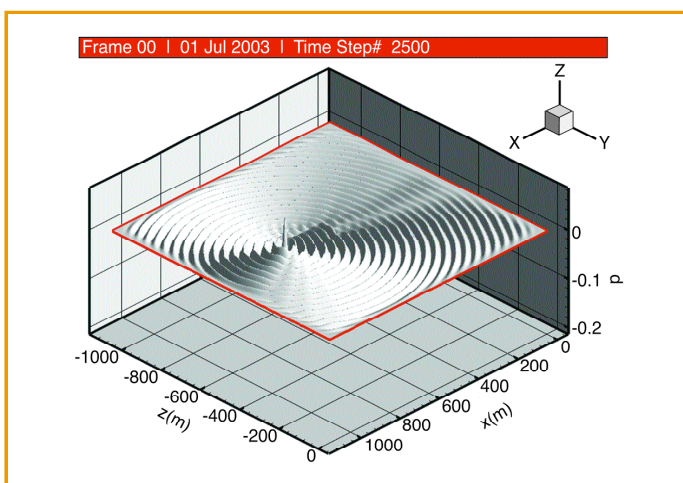Frame 00 | 01 Jul 2003 | Time Step# 2500

Figure 1. Snapshot of the pressure field generated by a 100 Hz pressure source located in the lower left corner of a homogeneous medium with a single fracture, located in the middle of the model. An anisotropic, viscoelastic, time-domain staggered grid was used in this computation.

CLAY MINERAL SURFACE GEOCHEMISTRY: STRUCTURE OF WATER ADSORBED ON A MICA SURFACE

Sung-Ho Park and Garrison Sposito
Contact: Sung-Ho Park, 510/643-372, sungho_park@lbl.gov

RESEARCH OBJECTIVES

The objective of this project is to obtain the detailed structural properties of hydration water on a micaceous mineral surface.

APPROACH

Our approach uses Monte Carlo simulations as implemented in the program MONTE. The Muscovite model formula, $K_{16}Al_{23}(Al_{16}Si_{48})O_{160}(OH)_{32}$ was used with 256 water molecules in a simulation cell. This cell was then replicated infinitely in three dimensions to mimic a macroscopic mica-water interface system. The model potential functions used to represent water-water, counterion-water, counterion-counterion, counterion-mineral, and water-mineral interactions have been tested extensively and successfully for 2:1 clay-mineral hydrates. Our simulations were performed in a constant (NsT) ensemble, in which absolute temperature (T) and pressure applied normal to the mineral layers (s) are maintained at 300 K and 100 kPa, respectively.

ACCOMPLISHMENTS

We have ascertained the detailed molecular structure of the mica-water interface. Figure 1 compares the water O (oxygen) density profile we obtained by Monte Carlo simulation with that derived from x-ray reflectivity measurements (Cheng et al., 2001). The match between their profile and ours (within 4 Å from the surface O) is excellent, encouraging a direct interpretation of the two principal features in terms of adsorbed water species, as predicted by our simulation. The first peak in the O density profile describes the water molecules adsorbed near ditrigonal cavities, while the second peak corresponds to adsorbed water molecules distributed laterally at approximately 1.3 per surface cavity, as also reported by Cheng et al. (Figure 1). Visualization showed that most of these water molecules are oriented with one of their OH groups pointing toward the mineral-surface O, which is consistent with hydrogen bond formation.

SIGNIFICANCE OF FINDINGS

Our simulation results were consistent with liquid-like disorder for the hydrate as a whole (Cheng et al., 2001) on the basis of their water O density profile tending to approach the bulk liquid limit after only a few oscillations (Figure 1). Overall, the structure of water adsorbed by micaceous minerals appears to be significantly more disordered than that of ice Ih. Our Monte Carlo results may also help to clarify the molecular interpretation of recent surface-force balance experiments involving hydration water between mica surfaces (Reviv et al., 2001). These experiments indicate that K+ counterions are displaced into the hydration layers, in agreement with our simulation results; that a single layer of strongly adsorbed water may exist at the mica surface, in agreement with Figure 1; and that hydration water films thicker than about 4 Å are liquid-like.

RELATED PUBLICATIONS

Cheng, L., P. Fenter, K.L. Nagy, M.L., Schlegel, and N.C. Sturchio, Molecular-scale density oscillations in water adjacent to a mica surface. Phys. Rev. Lett. 87, 156103, 2001.

Reviv, U., P. Laurat, and J. Klein, Fluidity of water confined to subnanometre films. Nature, 413, 51, 2001.

Park, S.-H. and G. Sposito, Do montmorillonite surfaces promote methane hydrate formation?: Monte Carlo and molecular dynamics simulations. J. Phys. Chem. B. 107, 2281, 2003.

Park, S.-H. and G. Sposito, Structure of water adsorbed on a mica surface. Phys. Rev. Lett. 89, 85501, 2001. URL: http://esd.lbl.gov/GEO/aqueous_geochem/index.html.
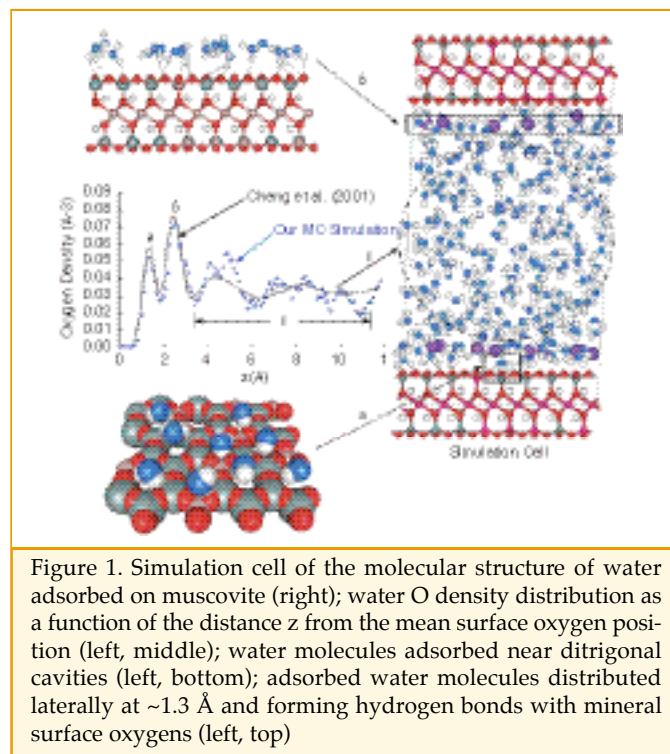
Figure 1. Simulation cell of the molecular structure of water adsorbed on muscovite (right); water O density distribution as a function of the distance z from the mean surface oxygen position (left, middle); water molecules adsorbed near ditrigonal cavities (left, bottom); adsorbed water molecules distributed laterally at ~1.3 Å and forming hydrogen bonds with mineral surface oxygens (left, top)

ACKNOWLEDGMENTS

INTERCOMPARISON OF SIMULATION CODES FOR GEOLOGIC SEQUESTRATION OF CO_2

Karsten Pruess

Contact: 415/486-6732, k_pruess@lbl.gov

RESEARCH OBJECTIVES

Mathematical models and numerical simulation tools play an important role in evaluating the feasibility of CO_2 storage in subsurface reservoirs, such as brine aquifers, producing or depleted oil and gas reservoirs, and coalbeds. We have designed and performed a code intercomparison study to explore the capabilities of numerical simulators to accurately and reliably model the important physical and chemical processes that would be taking place in CO_2 disposal systems. The overall objective of the study is to document and advance the state of the art in modeling CO_2 injection into subsurface reservoirs, and to establish credibility for currently available modeling approaches.

APPROACH

Berkeley Lab designed and directed the code intercomparison study. A set of eight test problems was assembled to examine flow processes during CO_2 injection into brine formations, depleted gas reservoirs, and oil reservoirs. Key issues addressed in these problems include (1) the thermodynamics of sub- and supercritical CO_2, and PVT properties of mixtures of CO_2 with other fluids, including (saline) water, oil, and natural gas; (2) the fluid mechanics of single and multiphase flow when CO_2 is injected into aquifers, oil reservoirs, and natural gas reservoirs; (3) coupled hydrochemical effects caused by interactions among CO_2, reservoir fluids, and primary mineral assemblages; (4) coupled hydromechanical effects, such as porosity and permeability change, caused by increased fluid pressures from CO_2 injection; and (5) space and time discretization effects. The test problems were distributed to interested groups of scientists and engineers, and the Internet was used as a convenient vehicle to help organize this effort.

ACCOMPLISHMENTS

Ten groups from six countries participated in the study, including Berkeley Lab, Stanford University, Lawrence Livermore National Laboratory, Los Alamos National Laboratory, Pacific Northwest National Laboratory, Alberta Research Council (Canada), Industrial Research Ltd. (New Zealand), CSIRO Petroleum (Australia), University of Stuttgart (Germany), and the Institut Français de Pétrol (France).

In the course of the study, a number of bugs were found and corrected in several simulation codes. Substantial agreement was achieved between results predicted from different simulators, but there exist areas with only fair agreement, as well as some significant discrepancies. Most discrepancies could be traced to differences in fluid property descriptions, an area that will clearly require continuing efforts by code developers to assure that realistic results can be obtained. Some disagreements were caused by effects from space and time discretization, while occasionally discrepancies were noted for which no rational explanation could be found.

A full presentation and discussion of results submitted by all groups are given in a laboratory report (Pruess et al., 2002). A separate report with a more detailed presentation of Berkeley Lab results for the saline-brine-formation problems is also available (Pruess and García, 2002). These reports, as well as other related materials, are available on the Web at http://www-esd.lbl.gov/GEOSEQ/.

SIGNIFICANCE OF FINDINGS

Although code development work undoubtedly must continue, this work has shown that codes are available now that can robustly model the complex phenomena accompanying geologic storage of CO_2, and with quantitatively similar results.

RELATED PUBLICATIONS

Pruess, K., and J. García. Solutions of test problems for disposal of CO_2 in saline aquifers. Berkeley Lab Report LBNL-51812, 2002.

Pruess, K., J. García, T. Kovscek, C. Oldenburg, J. Rutqvist, C. Steefel, and T. Xu, Intercomparison of numerical simulation codes for geologic disposal of CO_2. Berkeley Lab Report LBNL-51813, 2002.

Pruess, K., C.F. Tsang, D. H.-S. Law, and C.M. Oldenburg. Intercomparison of simulation models for CO_2 disposal in underground storage reservoirs. Berkeley Lab Report LBNL-47353, 2000.

ACKNOWLEDGMENTS

INVESTIGATION OF THE EFFECTS OF EVAPORATION AND INFILTRATION ON VADOSE ZONE PORE-FLUID $\delta^{18}O$ VALUES AT HANFORD, USING TOUGHREACT

Michael J. Singleton, Eric L. Sonnenthal, Donald J. DePaolo, and Mark E. Conrad
Contact: Michael Singleton, 510/486-5241, mjsingleton@lbl.gov

RESEARCH OBJECTIVES

The fraction of rainfall that percolates deep into the vadose zone in arid regions is difficult to predict, but important for understanding groundwater recharge and contaminant transport. At Hanford, where a large amount of radionuclide contamination is present in the vadose zone above the water table, it is especially important to know the water infiltration flux, because this determines how rapidly radionuclides will reach groundwater. This study is aimed at evaluating the use of numerical models in conjunction with water isotope data to measure infiltration flux in arid regions.

APPROACH

The vadose zone hydrological processes that control infiltration also generate variations in the ratios of stable isotopes (i.e., $^{18}O/^{16}O$ and $^2H/^1H$) in water and water vapor. A numerical modeling approach is needed to account for the interplay between evapotranspiration, advection, and diffusion. We implemented the temperature-dependent equilibration of stable isotopic species between water and water vapor, and their differing diffusive transport properties, into the thermodynamic database of the reactive transport code TOUGHREACT, developed at Berkeley Lab. This allows for the simulation of stable isotope fractionation in tandem with multiphase unsaturated flow, heat transport, mineral-water-gas reactions, and the transport of other gaseous and aqueous species.

ACCOMPLISHMENTS

TOUGHREACT simulations with isotope fractionation provide new insights into the behavior of water isotopes in unsaturated zone pore waters in semi-arid climates. Preliminary results (Figure 1) emphasize the effects of alternating wet and dry seasons, which lead to annual fluctuations in moisture content, capillary pressure, and stable isotope compositions in the vadose zone. The effective depths of evaporation and wetting events are primarily controlled by soil properties and infiltration rate. Repeated annual cycles of wet and dry seasons in a semi-arid climate lead to a consistent shift in the isotopic composition of deep vadose zone pore waters, which is proportional to the amount of infiltration.

SIGNIFICANCE OF FINDINGS

Stable isotope profiles provide a dynamic record of evaporation and infiltration in the unsaturated zone. For the range of infiltration rates measured at the Hanford Site (5–200 mm/yr), stable isotope profiles are affected by surface conditions on annual-to-decadal time scales, and therefore can provide a record of recent events such as

dumped or spilled waste water, soil removal, and devegetation by brush fires. Numerical simulations of transport and isotope fractionation using TOUGHREACT provide a method to quantitatively interpret the relationship of stable isotope depth profiles to infiltration rate.
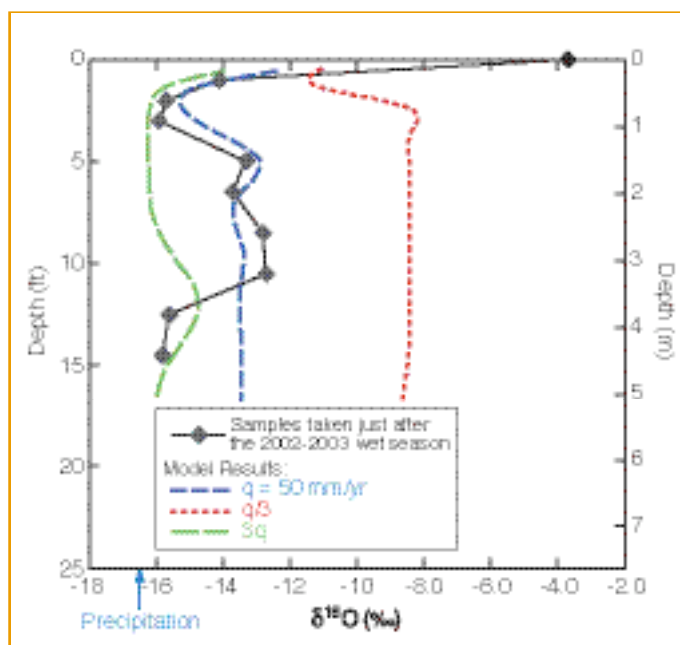
Figure 1. Model results for a vertical Hanford Site vadose zone profile of oxygen isotope compositions with different infiltration rates (q), compared with pore-water samples taken just after the wet season from a lysimeter where the infiltration rate is known to be 55 mm/year

URANIUM DIFFUSION

Tetsu K. Tokunaga, Jiamin Wan, Jasquelin Pena, Stephen R. Sutton[1], and Matt Newville[1]
[1]University of Chicago
Contact: Tetsu Tokunaga, 510/486-7176, tktokunaga@lbl.gov

RESEARCH OBJECTIVES

Transport of uranium (U) in contaminated soils and sediments is of great concern. Environments affected by U contamination can be very challenging to understand because extreme disequilibrium is likely in such environments, especially during early stages of waste migration, when solutions are still often either highly acidic or highly alkaline. The impact of diffusion is especially important when large fractions of the subsurface have low hydraulic conductivities relative to a small fraction of interconnected preferential flow paths, and where hydraulic gradients are low. In this study, we are concerned with diffusion of U(VI) species, since these are commonly much more soluble and mobile than U(IV) species. Because U(VI) forms a variety of strongly pH-dependent solution complexes and surface complexes, its sorption—and thus its mobility—is strongly pH-dependent. Experiments are being conducted to test various models for predicting transient U(VI) diffusion.

APPROACH

Measurements were obtained on U(VI) diffusion into two different soil types, one neutral and the other slightly alkaline. To each of these soil types, we applied U(VI) solutions, one acidic and the other alkaline. Periodic measurements of redox potential profiles within the soil columns, and of pH and U concentrations in the boundary reservoirs, were obtained. Profiles of the total U and U(VI) distribution in the sediment column were obtained by micro- x-ray absorption near-edge structure (micro-XANES) spectroscopy. Measured U profiles were compared with various model predictions.

ACCOMPLISHMENTS

Micro-XANES analyses confirm that U remains in oxidized U(VI) forms within systems having low organic carbon availability. Strong pH-dependent apparent U(VI) diffusivities are obtained in transient experiments. These apparent diffusivities are in fair agreement with predictions based on aqueous-phase U(VI) diffusivities, soil porosities, and pH-dependent sorption isotherms. Ongoing sorption studies (Zheng et al., 2003) are being conducted through a related NABIR-supported project.

SIGNIFICANCE OF FINDINGS

Predicting the mobility of U in soils and sediments requires an understanding of its diffusive transport. Such understanding is being provided in this study, through direct measurements of U(VI) diffusion profiles and comparisons with U(VI) sorption isotherms.

RELATED PUBLICATIONS

Tokunaga, T.K., J. Wan, T.C. Hazen, E. Schwartz, M.K. Firestone, S.R. Sutton, M. Newville, K.R. Olson, A. Lanzirotti, and W. Rao, Distribution of chromium contamination and microbial activity in soil aggregates. J. Environ. Qual. 32, 541–549, 2003.

Zheng, Z., T.K. Tokunaga, and J. Wan, Influence of calcium carbonate on sorption of U(VI) to soils. Environ. Sci. Technol., 2003.
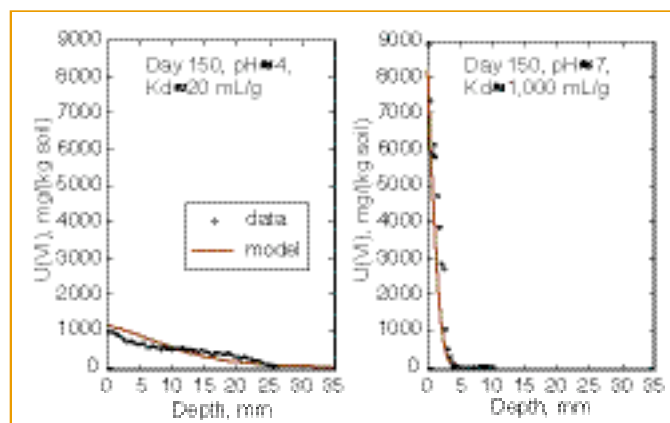
ACKNOWLEDGMENTS

Figure 1. Micro-XANES profiles at day 150, for U(VI) diffusing into Oak Ridge soil from initially acidic (left) and initially alkaline (right) solutions. Neutralization of the alkaline system resulted in strong U(VI) sorption and retardation of the diffusion front. Model calculations are based on measured porosities, aqueous-phase U(VI) diffusivities, and pH-dependent U(VI) sorption.

VANISHING OF CAPILLARY HYSTERESIS IN POROUS MEDIA

Tetsu K. Tokunaga, Keith R. Olson, and Jiamin Wan
Contact: Tetsu K. Tokunaga, 510-486-7176, tktokunaga@lbl.gov

RESEARCH OBJECTIVES

The degree of water saturation (S) exerts strong influences on water flow, transport of solutes and heat, and mechanical properties of porous media. The monotonic decrease of the matric potential (ψ) with decreased saturation reflects the combination of capillary and adsorptive influences in lowering the free energy of soil water. In the early decades of soil physics, it was assumed that the S(ψ) relation in a given system represented a series of unique equilibrium conditions. Since the classic 1930 paper of Haines, hysteresis in S(ψ) has been regarded as a basic aspect of interactions between water and variably saturated porous media. At any given potential, the equilibrium saturation level obtained by draining a system is greater than or equal to that obtained by wetting an initially dry system to the same potential. In an attempt to gain a better understanding of the hysteresis phenomenon, we consider conditions that lead to its disappearance.

APPROACH

Capillary models and Miller-Miller unsaturated hydraulic scaling were used to predict conditions necessary for removal of hysteresis. Disappearance of hysteresis was tested through suction plate measurements of drainage and wetting curves for sands and gravels, with grain sizes ranging from 0.2 to 14 mm. The influence of surface tension was tested through measurements of S(ψ) in 7 mm gravel, with and without a surfactant—sodium dodecylbenzenesulfonate (SDBS).

ACCOMPLISHMENTS

Calculations based on a simple pore-size model lead to the predicted disappearance of hysteresis in the grain-size range of 8 to 15 mm. A more constrained predicted grain-size limit of 10.4 ± 0.5 mm was obtained by applying Miller-Miller scaling to a conceptual model of Haines. More generally, hysteresis is also predicted to depend on surface tension, fluid densities, and acceleration. Laboratory measurements showed that hysteresis loops remain well defined for grain sizes up to 7 mm. At a grain size of 9 mm, hysteresis is barely detectable. For grain sizes equal to or greater than 10 mm, hysteresis is not observed. Measurements of S(ψ) on 7 mm gravels exhibited hysteresis without SDBS, but did not exhibit hysteresis with it. These results support our general analysis, which predicted elimination of hysteresis based on fluid densities, acceleration, grain size, and surface tension. These parameters combine to yield the dimensionless Haines number, with a critical value of 14.8 ± 1.4. Above this value, capillary hysteresis is not possible.

SIGNIFICANCE OF FINDINGS

The experiments completed in this project support the predicted grain-size and surface-tension dependence of capillary hysteresis, and show that hysteresis is not a fundamental feature of unsaturated porous media. Lack of previous awareness of nonhysteretic S(ψ) appears to result from the fact that the considered combinations of grain size, surface tension, fluid densities, and acceleration were within the realm in which capillary rise is greater than the grain size. Studies on unsaturated media conducted with surfactants and/or in centrifuges may benefit from this work.
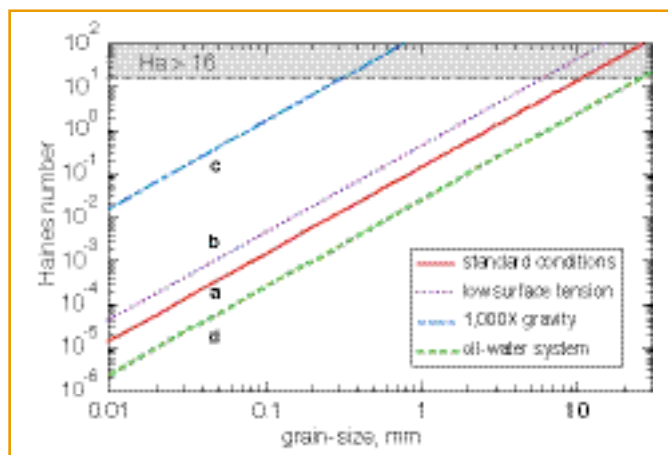

Figure 1. The Haines number is comprised of fluid-fluid density differences and surface tension, acceleration, and grain-size. Grain-size dependence of the Haines number for (a) standard conditions (air-water, ordinary gravity), (b) low surface tension (surfactant solution, ordinary gravity), (c) much higher body force (air-water, 1,000g centrifuge), and (d) an oil-water system conditions (ordinary gravity). The horizontal line at *Ha* = 16 separates systems that do and that do not exhibit hysteresis.

RELATED PUBLICATIONS

Tokunaga, T.K., J. Wan, and K.R. Olson. Saturation-matric potential relations in gravel. Water Resour. Res. 38(10), 1214, doi:10.1029/2001WR001242, 2002.

Tokunaga, T.K., K.R. Olson, and J. Wan. Moisture characteristics of Hanford gravels: Bulk, grain-surface, and intragranular components. Vadose Zone J., 2003 (in press).

ACKNOWLEDGMENTS

Helium Isotope Ratios in South Sister Volcano Vicinity, Cold Springs

Matthijs C. van Soest, B. Mack Kennedy, William C. Evans[1], Robert H. Mariner[1], and Mariek E. Schmidt[2]
[1]U.S. Geological Survey, Menlo Park, California
[2]Department of Geosciences, Oregon State University, Corvallis, Oregon
Contact: Matthijs C. van Soest, 510/486-5659, mcvansoest@lbl.gov

RESEARCH OBJECTIVES

As part of a geochemical monitoring project at Oregon's South Sister volcano—a volcano that is undergoing strong uplift (Wicks et al., 2002)—we are carrying out a detailed study of helium isotope ratios in cold and hot springs in the Separation Creek drainage area. Through this study, we hope to determine the occurrence of any changes in spring chemistry that could be related to the ongoing uplift.

APPROACH

Helium isotope ratios (^{3}He/^{4}He) in fluids from volcanic areas are useful indicators for the presence of a magmatic component in those fluids. Moreover, in combination with other geochemical indicators, these ratios are indicative of a magma source and subsequent chemical processing of the fluids. The approach of this project was two-fold: (1) to establish a baseline of helium isotope ratios for springs within the zone of uplift and the surrounding area, and (2) establish a chemical and isotopic monitoring program for selected springs within the area.

ACCOMPLISHMENTS

Helium isotope data from the Three Sisters area are shown in Figure 1a. All the springs in the area, hot or cold, show a significant magmatic helium component. The most remarkable results are that two cold springs with a free gas phase, one close to the center of the uplift zone and the other close to the volcanic edifice itself, gave helium isotope ratios that are indistinguishable from pristine upper-mantle-derived helium (8 ± 1 times RA, where RA is the ratio in air and used for normalization). For the rest of the area, the data show a general trend of decreasing helium isotope ratios with distance from the zone of uplift (Figure 1b). This trend reflects dilution of the magmatic helium component with crustal fluids that typically are rich in radiogenic ^{4}He (^{3}He/^{4}He ~ 0.02 RA).

During the time this study was conducted, none of the monitored springs showed any significant changes (Figure 1a) in helium isotopic composition. To further understand the system, we are continuing the monitoring program.

SIGNIFICANCE OF FINDINGS

Geochemical explorations for deep hot fluids, of economic interest as a potential energy source, generally focus on hot springs to the exclusion of nonthermal waters. The surprisingly very high helium isotopic compositions observed in two of the cold springs suggests that cold springs should not be overlooked, because they may contain helium isotope signatures reflecting deep processes, such as magma intrusion, that precede thermal and/or chemical pulses at the surface.
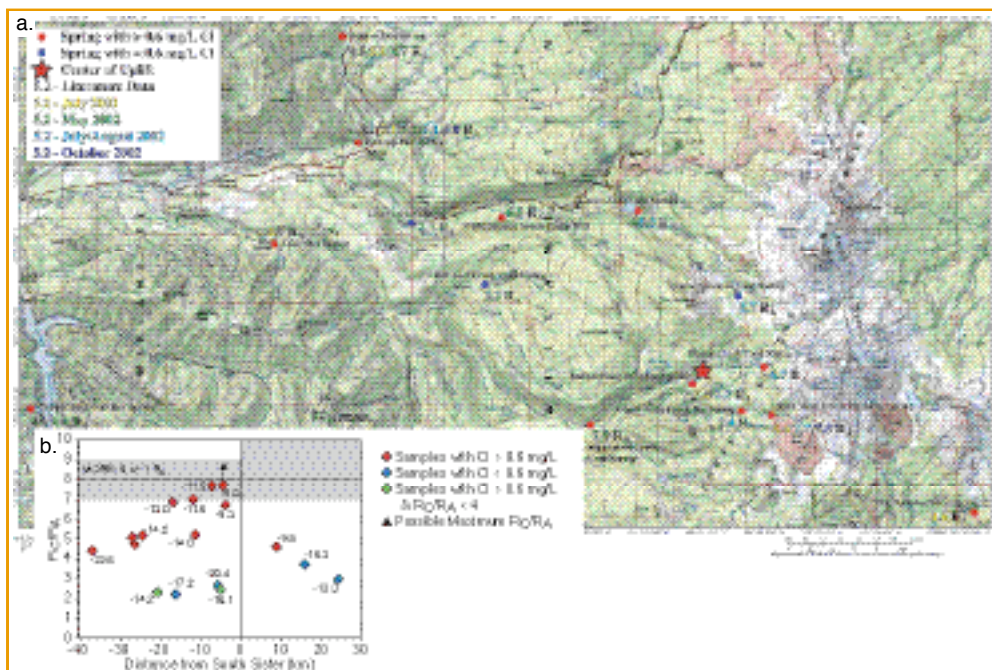

Figure 1(a). Overview map of the Three Sisters area, central Oregon, with sample locations and helium isotope results, using color coding for sampling date and general spring chemistry indication; (b) Plot of helium isotope ratio vs. distance from the volcano, with δ^{13}C values next to each data point showing a similar trend.

RELATED PUBLICATIONS

Wicks, C., Jr., D. Dzurisin, S.E. Ingebritsen, W. Thatcher, Z. Lu, and J. Iversen, Magmatic activity beneath the quiescent Three Sisters volcanic center, central Oregon Cascade Range, Oregon. Geophysical Research Letters, 29, 26-1–26-4, 2002.

ACKNOWLEDGMENTS

NANOPARTICLES IN SUBSURFACE ENVIRONMENTS: ABUNDANCE AND TRANSPORT OF THE MOBILE FRACTION

Jiamin Wan, Guilin Han, Jasquelin Pena, Xiang-Yun Song, and Tetsu Tokunaga
Contact: Jiamin Wan, 510/486-6004, jmwan@lbl.gov

RESEARCH OBJECTIVES

The earth science community has identified environmental nanoscience as an important emerging field. This project provides the first survey of mobile nanoparticle inventories for sediments from a variety of subsurface environments. The research will also provide systematic studies of subsurface nanoparticle transport and its dependence on nanoparticle, sediment, solution, and hydraulic characteristics.

APPROACH

Quantification of the potentially mobile nanoparticle inventory requires separation of nanoparticle size fractions. In this study, particles in the <100 nm size range are defined as nanoparticles. Methods such as flow-through columns, batch extractions in water, and batch extractions with a dispersant (sodium hexametaphosphate) are used. In these ways, operationally defined measures of mass and specific surface areas associated with different particle fractions will be obtained in several sediment types from DOE facilities across the country. Nanoparticle transport quantification will be performed through laboratory column experiments with three types of variables. These are (1) natural versus synthetic (glass bead) sediments, (2) natural versus synthetic (polystyrene latex) particles, and saturated versus unsaturated conditions. Through these experiments, the validity of filtration-theory predictions for nanoparticles will be tested.

ACCOMPLISHMENTS

Mobile nanoparticle inventories for two types of sediments were studied, one from the Hanford Site and another from Oak Ridge National Laboratory. Our results show that the release of mobile nanoparticles depends strongly on solution chemistry, including pH, ionic strength, and anions. The maximum particle release occurred at the lowest ionic strength condition. Alkaline pH favors particle release. For example, in the Oak Ridge sediments, the measured nanoparticle fractions (<0.1 μm) were 0.98% at pH 12.0, and the maximum release obtained with hexametaphosphate solution was 1.72%. The nanoparticle fraction is about 7% of the total clay fraction (<2.0 μm) released in this sediment. We have also discovered that some U(VI) nanoparticles are relatively stable in the pore solutions of contaminated Hanford sediment (as shown in Figure 1). Uranium(IV) nanoparticles have been found in the mine drainage waters as a result of microbial reduction. This species has previously been considered highly soluble under our test conditions, and thus we did not expect to find U(VI) nanoparticles in this contaminated Hanford system.

SIGNIFICANCE OF FINDINGS

This research provides the first survey of mobile nanoparticle inventories for sediments from a variety of subsurface environments. It will also provide systematic studies of subsurface nanopartide transport and its dependence on nanoparticle, sediment, solution, and hydraulic characteristics. The transport experiments will also be the first to test the validity of filtration theory for nanoparticles in the subsurface.

RELATED PUBLICATIONS

Wan, J., G. Han, J. Pena, X.Y. Song, and T.K. Tokunaga, The natural abundance of nanoparticles in soils. J. Colloid Interface Sci., 2003 (submitted).

Wan, J., J. Pena, X.Y. Song, Z. Zheng, and T.K.Tokunaga, U(VI) nanoparticles in calcium carbonate-rich subsurface environment. Environ. Sci. Technol., 2003 (submitted).
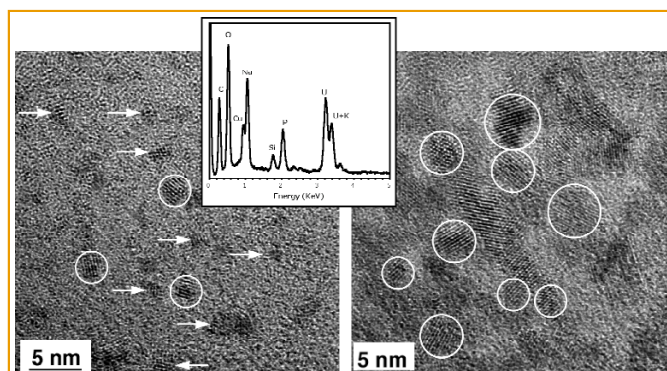
ACKNOWLEDGMENTS

Figure 1. U(VI) nanoparticles (marked by arrows and circles) obtained from a pore solution of U contaminated sediment. Based on lattice fringe (by TEM) and elemental composition (by EDX) analyses, the particles are identified as sodium uranium oxide phosphate hydrate, $Na_4U_3O_8(PO_4).6H_2O$ (Wan et al., unpublished).

Comparison of the Wet Hematite and Corundum (0001) Surface Structures Determined by Synchrotron X-Ray CTR Analysis

Glenn Waychunas, Thomas Trainor[1], Peter Eng[1], and Gordon Brown[2]
[1]University of Chicago and Advanced Photon Source, Argonne National Laboratory
[2]Stanford University, Stanford, California
Contact: Glenn Waychunas, 510/495-2225, gawaychunas@lbl.gov

RESEARCH OBJECTIVES

The surfaces of crystalline minerals generally differ from the bulk structure due to atomic relaxation, expansion, or rearrangement. These changes can have profound effects on the reactivity of the mineral, especially with regard to toxics sorption, catalytic activity, and dissolution. Although modern thermodynamic calculations and structural simulations are now well developed, these still rest on the fundamental underpinning of the experimental determination of the true surface structure. Here we focus on two isostructural phases that behave quite differently in the environment. Hematite is a primary soil mineral with much greater reactivity than corundum. Though itself not found in soils, the corundum (0001) surface structure is a much-used analog for the alumina layers in clays, which also have relatively low reactivity. The aim is to uncover a structural basis for the differences in reactivity.

APPROACH

We use crystal truncation rod (CTR) surface x-ray diffraction to probe the atomic positions at the surfaces of highly perfect corundum and hematite (0001) crystals under water solutions. Current work utilizes near-neutral water, but will also examine the effect of pH on surface structure. The technique is based on the fact that the crystal surface termination produces streaks (or "rods") in diffraction space perpendicular to the surface. Though they are of low intensity, equivalent to the scattering of a half-plane of atoms, these rods can be quantitatively measured by synchrotron x-ray diffraction. Small changes in the atomic occupations or positions can have large effects on the rod intensities at different positions in diffraction space, and hence the rod measurements can be refined to reveal the atomic structure of the surface.

ACCOMPLISHMENTS

Our original CTR analysis of the corundum (0001) surface (Eng et al., 2000) shows considerable relaxations of surface atoms down more than 6 atomic layers. The most important aspect is the shift in the aluminum metal ions near the surface towards the gibbsite (AlOOH) structure. An organized layer of sorbed water
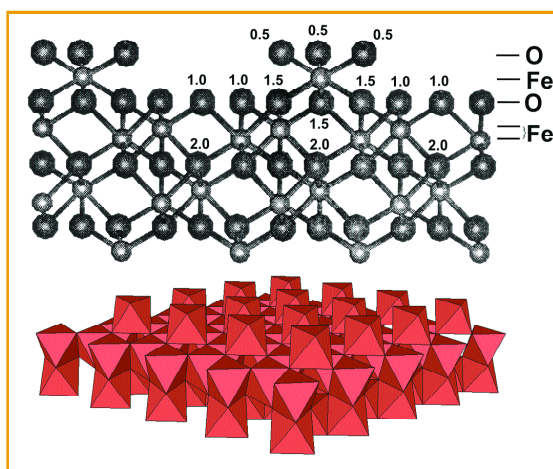

Figure 1. Proposed structure of the hydrated (0001) hematite surface: top: ball and stick structure showing Fe atoms and associated bond valences (inversely related to reactivity); bottom: idealized polyhedral model of the surface. Each octahedron is a FeO_6 unit.

is also present. Finally, the surface is perfectly terminated by oxygen ions and the water layer. In the hematite (0001) surface, the results are similar (see Figure 1), but individual iron ions with surrounding oxygens form islands on the surface. These islands allow for lower-coordination attachment points for reacting species, unlike the smooth corundum surface that presents only fully coordinated (saturated) metal sites. This sort of result may be a general reason for enhanced reactivity at particular metal oxide mineral surfaces. Analogous work on sorption on the same mineral surfaces using GIXAFS techniques (Waychunas, 2002) supports and confirms our results.

SIGNIFICANCE OF FINDINGS

Besides the important and fundamental connection of reactivity to structure, the work helps to improve our simulation capability for model-reactive-metal-oxide mineral surfaces. The interatomic potentials used for such simulations—usually molecular dynamics—can be adjusted so that computer results closely approximate the experimental surface structures. Then the simulations can be applied with greater confidence to other mineral-water systems, such as goethite-water.

RELATED PUBLICATIONS

Eng, P.J., T.P. Trainor, G.E. Brown, G.A. Waychunas, M. Newville, S.R. Sutton, and M.L. Rivers, Structure of the hydrated a-Al_2O_3 (0001) surface. Science, 288, 1029–1033, 2000.

Waychunas, G.A., Grazing-incidence X-ray absorption and emission spectroscopy. Reviews in Mineralogy and Geochemistry, 49, 267–315, 2002.

ACKNOWLEDGMENTS

Manganese Valence and Mineral Surface Structure Determined with In Situ Soft X-Ray Spectroscopy

Glenn Waychunas, David Shuh, and Mario Villalobos
Contact: Glenn Waychunas, 510/495-2224, gawaychunas@lbl.gov

RESEARCH OBJECTIVES

Manganese (Mn) minerals have high surface reactivity, redox potentials that can either reduce or oxidize adsorbed species, and high surface areas (fine grain sizes). These aspects make them extremely significant players in metal sequestration due to strong sorption and alteration in valence states (and hence solubility products) of solution species. Our goals are to determine how much information about Mn valence states and surface structure (i.e., surface mineral phase) can be extracted from K-edge oxygen and L-edge manganese x-ray fluorescence spectra, measured at the Advanced Light Source (ALS) at Berkeley Lab.

APPROACH

Experiments are designed to investigate both dry ultra-high-vacuum (UHV) mineral surfaces and surfaces in equilibrium with ambient water pressures. Fifteen different Mn mineral samples (both synthetic and natural) were examined at ALS Beam Line 9.3.2, using both photon yield and photoelectron yield, allowing simultaneous analysis of bulk and surface (5 nm) chemistry and structure.

ACCOMPLISHMENTS

Some representative spectra from our work are shown in Figure 1. Each valence state of Mn has well-defined features on the L-edge as well as a progressive shift in edge position. Accurate measurement (to about 1% relative) of valence ratios are possible for these models when two valence states are present. All phases showed the same bulk and surface valences, except for manganite (nominally Mn^{3+} with composition $MnOOH$), which has an oxidized surface.

The structure of the Mn phase has less effect on the Mn L spectra than it does on the O K-edge spectra. This is because the Mn L-edge transitions are mainly crystal field transitions, while the O K-edge transitions include multiple scattering, extended x-ray absorption fine structure (EXAFS), and valence-shell bound state features. This allows the two types of spectra, which can be collected in the same spectroscopy scans, to be used complementarily. For example, the manganite surface coating, less than 5 nm thick, appears to be mainly ramsdellite-like.

SIGNIFICANCE OF FINDINGS

These spectroscopy tools can be used to determine the precise chemical reactions at Mn mineral surfaces and whether redox reactions are occurring. Redox reactions can alter the solubility and thus transportability of any surface-sorbed contaminant. In many waste situations, for example at Yucca Mountain, Nevada, small amounts of Mn phases can have large effects on contaminant sequestration. Hence, this type of analysis is crucial to a complete understanding of the ultimate fate of contaminants in Mn mineral-containing environments.
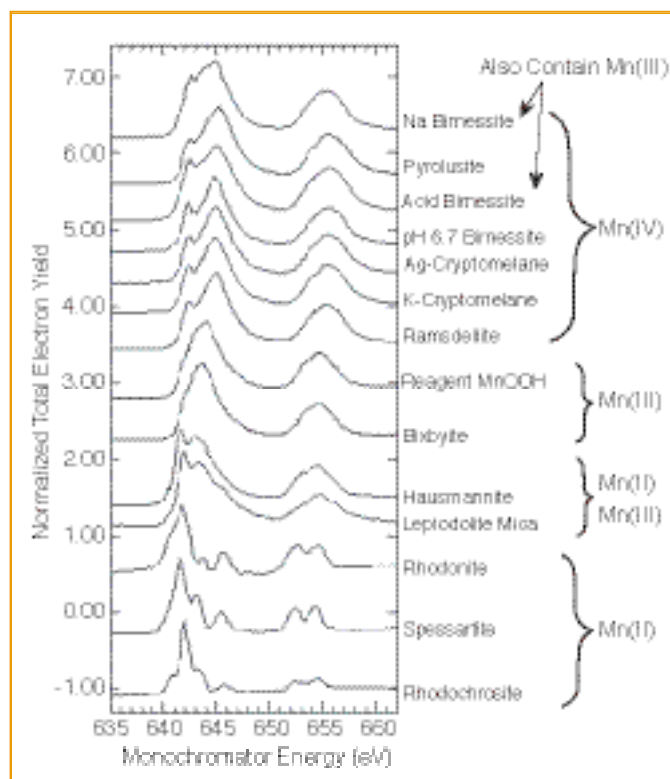
ACKNOWLEDGMENTS

Figure 1. Mn L-edge fluorescence spectra for Mn minerals with different structures and valences. The differences in the Mn (II) spectra result from the varied coordination environments of Mn in each mineral (rhodochrosite—6 coordinated; spessartite—8 coordinated; rhodonite—5 and 6 coordinated). Both features and energy positions are characteristic of the Mn valence state.

SUM-FREQUENCY SPECTROSCOPIC STUDIES OF MINERAL–WATER INTERFACES

Glenn A Waychunas, Victor Ostroverkhov, and Y. Ron Shen
Contact: Glenn A. Waychunas, 510/495-2224, gawaychunas@lbl.gov

RESEARCH OBJECTIVES

Interactions of water and aqueous solutions with mineral surfaces play an important role in a variety of environmental processes. These processes include soil formation, cycling of chemical elements in nature, mobility of heavy metals and other contaminants as well as nutrients, and surface growth of microorganisms (Brown et al., 1999). Such interactions are affected by solution pH, the presence of dissolved ions, and the surface structure of the solid. The objective of this project is to use available experimental techniques and theoretical approaches to develop a comprehensive microscopic picture of how water and solutes interact with mineral surfaces.

APPROACH

To study the structure of water at a mineral surface, we use sum-frequency vibrational spectroscopy—a surface-specific technique with monolayer sensitivity that can be applied under ambient conditions (Shen, 1989). The technique is based on sum-frequency generation (SFG), a second-order nonlinear optical process in which two intense input laser beams focused on the medium produce an output beam at the frequency $\omega=\omega_1+\omega_2$. The process is electric-dipole allowed only in noncentrosymmetric media, and thus it is capable of probing the molecular ordering at the interface caused by the breaking of centrosymmetry at the surface. One of the input beam frequencies is tunable in the range of system vibrational resonances (e.g., water molecule vibrations or metal-oxygen stretching vibrations). Hence, spectroscopic information is obtained from the water layer just at the surface, from which the orientational distribution and structural type of molecular species can be extracted.
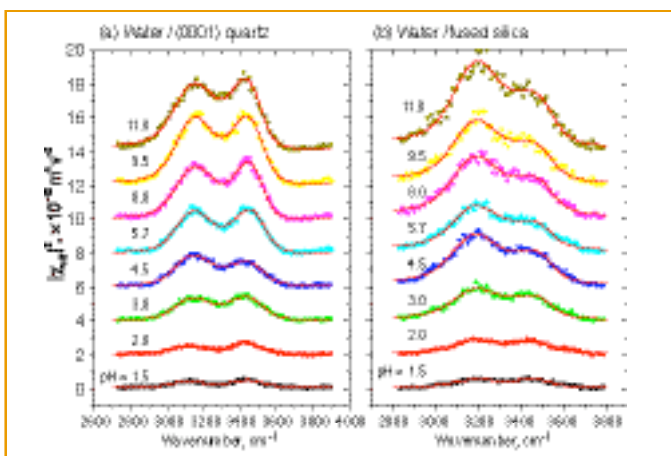

Figure 1. Sum frequency vibrational spectra for water on (a) (0001) alpha quartz surface and (b) vitreous silica surface as a function of pH. The lower energy peak is due to ice-like structure water, while the higher energy peak is due to water forming several hydrogen bonds.

ACCOMPLISHMENTS

In the past, SFG has been used to observe ice-like ordering of water molecules on a vitreous silica surface (Du et al., 1994). Here, for the first time we implement sum-frequency vibrational spectroscopy to extend the study to the interface of liquid water and a well-characterized surface (0001) of crystalline quartz (α-SiO$_2$)—one of the most abundant minerals. We have developed an experimental technique to differentiate a weak SFG signal from a strong background SFG generated in the bulk of quartz crystal (a well-known nonlinear crystal) by use of special experiment geometry and light polarization combinations. Sets of interface water vibrational spectra as a function of pH have been obtained (Figure 1). Comparison with the case of vitreous silica shows that the crystallinity of the surface results in a higher degree of ordering in the interfacial layers of water at a given pH. This is shown by a pronounced red-shifting of the peak associated with the symmetrically (ice-like) coordinated species in the hydrogen bond network of water. With increasing pH, this peak also increases in intensity in both series, reflecting increasing surface negative charge. The data suggest that differing crystallographic surfaces may induce specific variations in water structure in the first few layers, as well as modification of response to pH and sorbing species.

SIGNIFICANCE OF FINDINGS

The measurements provide important information on the microscopic behavior of water in contact with the surface of α-quartz under ambient conditions, and suggest that water on specific mineral surfaces may differ in structural details. This could in part explain the variations of reaction rates on particular mineral surfaces. The study also provides additional constraints for potentials used in molecular-dynamic simulations of water on mineral surfaces, and has allowed enhanced interpretation of sum-frequency spectral features.

RELATED PUBLICATIONS

Brown, G.E., et al., Metal oxide surfaces and their interactions with aqueous solutions and microbial organisms. Chem. Rev., 99(1), 77–174, 1999.

Shen, Y.R., Surface-properties probed by 2nd-harmonic and sum-frequency generation. Nature, 337, 519–525, 1989.

Du, Q., et al., Vibrational-spectra of water-molecules at quartz water interfaces. Phys. Rev. Lett. 72(2), 238–241, 1994.

ACKNOWLEDGMENTS